**PAPER • OPEN ACCESS**

# Characterising the effects of wind-driven rain on the thermophysical performance of cavity walls by means of a Bayesian framework

To cite this article: V Gori *et al* 2021 *J. Phys.: Conf. Ser.* **2069** 012053

View the article online for updates and enhancements.

# Characterising the effects of wind-driven rain on the thermophysical performance of cavity walls by means of a Bayesian framework

**V Gori[1,4], V Marincioni[2,3] and H Altamirano-Medina[2,3]**

[1] UCL Energy Institute, University College London, 10 Montague street, London WC1B 5BJ, United Kingdom
[2] UCL Institute for Environmental Design and Engineering, University College London, 14 Upper Woburn Place, London WC1H 0NN, United Kingdom
[3] UK Centre for Moisture in Buildings, Here East, 8-9 East Bay Lane, Queen Elizabeth Olympic Park, London E15 2GW, United Kingdom

**Abstract**. Cavity wall is one of the most common construction types in temperate maritime climates, including the UK. However, water penetration may lead to damp within the structure, freeze-thaw damage at the outer surface and a reduction in thermal resistance. The magnitude of wetting effects on the energy performance of cavity walls is still unclear, with potentially significant implications for climate-change-mitigation strategies. This paper investigates the thermophysical performance of uninsulated and insulated cavity walls and its degradation as the element is wettened. Experiments were performed in a hygrothermal laboratory where two cavity-wall specimens (one of which coated with external waterproofing treatment) were tested under a high wind-driven rain exposure. Changes in the thermophysical performance between dry and wet conditions were evaluated through U-value testing and Bayesian inference. Substantial U-value increase was observed for wet uninsulated specimens (compared to dry conditions); conversely, closer U-value ranges were obtained when insulated with EPS grey beads. Moreover, latent-heat effects through the external masonry leaf of the untreated specimen were predicted by the Bayesian framework. Results suggest a negligible efficacy of waterproofing surface treatments as strategies for the reduction of heat transfer within the element, and possible effects of these agents on the evaporative and drying process.

## 1. Background

Cavity wall is one of the most common construction types in the UK, and more generally in temperate maritime climates [1,2]. However, when built in areas with high exposure to wind-driven rain (WDR), their thermophysical performance may be degraded as the resulting water penetration is considered the most important moisture source affecting the performance of the building fabric [3]. While the use of unfilled cavity walls in WDR exposed areas was based on the idea that the open cavity would have helped draining the wet external leaf, the water accumulated in the structure may lead to freeze-thaw damage of the external surface, damp within the structure and a consequent increase in thermal transmittance [3]. However, information on water ingress in uninsulated and insulated cavity walls as

---

well as its effects on their energy performance is hardly available [2], resulting in uncertainties around the efficacy of strategies for climate-change mitigation such as cavity insulation and use of waterproofing treatments on the external surface of the element.

This paper aims at investigating the degradation of the thermophysical performance of wet uninsulated and insulated cavity walls (compared to dry conditions), through hygrothermal laboratory testing. Insights into the hygrothermal behaviour of two cavity-wall specimens (one of which treated with a waterproofing agent on the exterior surface) were gained by exploiting the advantages of dynamic thermal simulations and Bayesian frameworks [4], including physical interpretability of results and combination of previous knowledge with the information contained in the measurements.

## 2. Methodology

Laboratory testing and thermophysical-performance evaluation analysis were carried out to gather insights into the effects of water penetration due to WDR on cavity-wall elements in exposed areas.

### 2.1. Laboratory testing

Two cavity-wall specimens of approximately 1 m$^2$ (to nearest brick dimensions) and constituted of two masonry leaves in stretcher bond with an empty cavity of 75 mm were built and cured under controlled conditions for a minimum of six months. Modern bricks were selected based on an extensive review [5] aiming at ensuring comparable and representative performance across the specimens; Table 1 summarises the hygric properties of the bricks used. One of the specimens had the outer surface of the external wall leaf coated with a waterproofing agent (silane/siloxane blend cream), while the other was left untreated for reference.

**Table 1.** Hygric properties of the bricks selected for the construction of the cavity-wall specimens [6].

| Wall coating | Water vapour diffusion resistance coefficient μ [-] | Water absorption coefficient $A_{w,brick}$ [kg/m$^2$/s$^{0.5}$] |
|---|---|---|
| Untreated | 18.23 | 0.1908 |
| Silane/siloxane blend cream | 21.50 | 0.0013 |

The two specimens were placed side-by-side in the centre of a double environmental chamber. The cavity space of each specimen was perimetrally sealed with acrylic adhesive tape to minimise air flow. Insulation boards of the same thickness as the specimens were placed all around to minimise lateral heat and moisture transfer by filling the gaps between the specimens and the chamber walls. A daily dynamic temperature profile was repeated in the internal (18.4±1.5 °C) and the external (11.0±3.7 °C, truncated for temperatures <10 °C) chambers to simulate representative indoor and outdoor UK conditions.

Each specimen was instrumented with five Hukseflux HFP01 [7] heat flux plates (HFP) and four surface temperature thermistors [8], all wired to a DataTaker DT85 data logging system [9]. Two locations (referred to as "Top" and "Bot" in the following) were monitored on each specimen by positioning the HFP and temperature sensors vertically aligned and in line with each other on the two sides of the element (Figure 1). The fifth HFP was placed on the external surface of the specimens for reference. The sensing part of the HFPs and thermistors were located on brick stretchers. Additional type-T thermocouples were placed on the outer masonry leaf inside the cavity space (in line with the rest of the monitoring kit, Figure 1) and wired to a Campbell Scientific CR23X datalogger [10].

Heat flux measurements were taken before and after a WDR wetting sequence. Initially, three full days of data were recorded with the specimen walls just moved from the curing room and exposed to the internal and external temperature profiles only (referred to as "dry condition" in the following). Subsequently, a WDR wetting period of two days was started; during this period, the two vertically aligned HFPs on the external masonry leaf were detached to ensure a uniform water distribution and penetration through the brick surface.
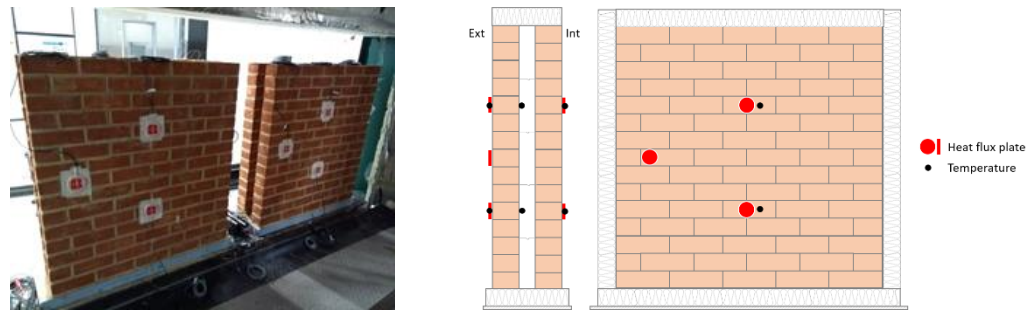
**Figure 1.** Instrumentation of the cavity-wall specimens in the environmental chamber before they were perimetrally sealed (left) and schematic of the monitoring equipment (right).

The WDR testing protocol was defined based on a review of test standards relating to exposure and water penetration of walls [5]. It consisted of 20-minute cycles of water spraying at a rate of 2.25 litres/m$^2$/minute followed by 40-minute rest; 2 cycles were performed on the first day while on the second day 2 further cycles were performed on the uninsulated configuration and 8 cycles on the insulated one, as the protocol was concluded when water was observed to penetrate the wall cavity and reach the inner leaf [11]. During this period, the temperature and relative humidity in both chambers were kept constant. At the end of the wetting period, the external HFPs were remounted in their original location and a second heat flux monitoring period (referred to as "wet condition" in the following) was started for three full days with the specimens exposed to the daily temperature profile above. The monitoring sequence was initially performed leaving the cavity space of the specimens empty, and subsequently repeated with the cavity space insulated with loose expanded polystyrene (EPS) grey beads. The polystyrene beads were poured into the cavity without adhesives and compacted until full, achieving a nominal average density of 14±2 kg/m$^3$ per installation to replicate industry guidelines. The specimens were stored in the curing room under controlled conditions between the uninsulated and insulated tests, until comparable initial interstitial conditions were observed [11].

*2.2. Data analysis*
The data analysis was undertaken using the dynamic Bayesian framework described in [4] to estimate the thermophysical properties of the two specimens under different configurations. Two lumped-thermal-mass models were implemented to simulate the heat transfer through the structure. The first model (3C4R) is constituted of three thermal capacitances and four thermal resistances (Figure 2); the initial temperatures of the three thermal masses are also parameters of the model.
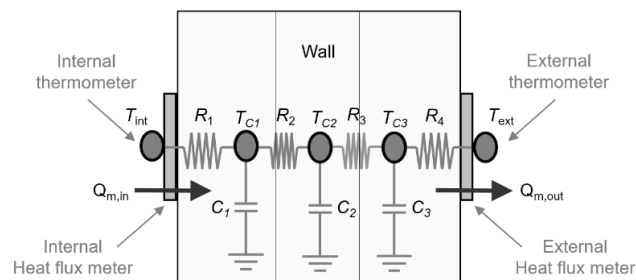


**Figure 2.** Three thermal capacitances and four thermal resistances model (3C4R). The diagram shows the equivalent electrical circuit modelling the heat transfer and the monitoring equipment.

The second model (3C3R) is parametrised by three thermal capacitances and three thermal resistances (Figure 3). It is built such that each thermal mass is located in the centre of each thermal resistance, assuming that each corresponds to the thermal resistance of a single layer. The initial temperature of the three thermal masses are also parameters of the model.
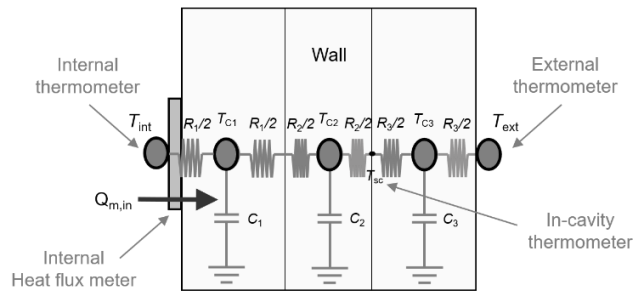
**Figure 3.** Three thermal capacitances and three thermal resistances model (3C3R). The diagrams show the equivalent electrical circuit modelling the heat transfer and the monitoring equipment.

For each model, the unnormalised posterior probability distribution of the parameters (i.e. the probability of the parameters $\theta$ given the observations $y$ and the model) was calculated assuming a multivariate Gaussian likelihood with zero mean and unknown covariance matrix $\Sigma_\varepsilon$, and a log-uniform improper prior on the parameters of the model (i.e. $\log \theta_i \sim \mathcal{U}(-\infty, +\infty)$ ). To account for temporal correlation between residuals, $\Sigma_\varepsilon$ was modelled as the covariance of a weakly stationary discrete-time random process. This allows approximating the covariance as $\Sigma_\varepsilon = D^{\mathrm{T}} \Xi_\varepsilon D$, where $D$ is the ortho-normal discrete cosine transform matrix and $\Xi_\varepsilon$ is a diagonal matrix [4]. A Gamma prior was placed on each diagonal element of $\Xi_\varepsilon$.

For both models, the internal and external surface temperatures were given as input to the model. For the 3C4R model, the internal and external heat flux observations were used to fit the parameters, while for the 3C3R model the internal heat flux and in-cavity temperature observations were used instead. Markov-chain Monte Carlo (MCMC) sampling was adopted to obtain samples from the posterior distribution and estimate the marginalised distribution of the parameters. The walkers were initialised using an overdisperse distribution centred at the maximum a posteriori (MAP). The Python library *EMCEE* was used for MCMC sampling while the Python SciPy *basinhopping* function was used for MAP optimisation [4]. The data were finally analysed with the average method [12] to compare the U-values obtained from the dynamic Bayesian framework with an established method.

## 3. Results and discussion

The data were initially analysed using the 3C4R model fitted with both the internal and external heat flux observations, as this configuration worked well in previous analyses [4,13]. Upon inspection, a peculiar behaviour was observed in the model's prediction of the heat fluxes and thermal mass temperatures for the wet untreated specimen (which was not replicated for the dry untreated, and the dry- and wet-treated ones). Specifically, while the model was fitting well both the interior and external heat flux observations, the temperature of the central thermal mass was constantly increasing over time during the analysis period (Figure 4 as an example; top location for the untreated and uninsulated specimen in wet conditions).
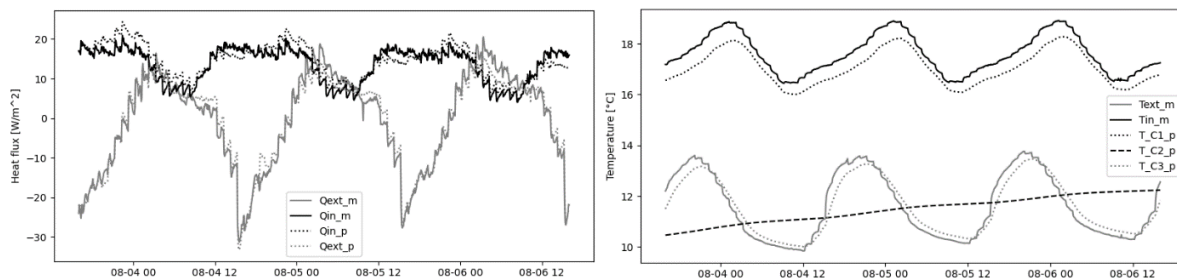


**Figure 4.** Internal and external heat flux (left) and temperature (right) measurements (indicated as _m) and model predictions (indicated as _p) in wet conditions (untreated specimen) using the 3C4R model.

After careful consideration, it was concluded that this behaviour was an attempt by the model to account for the fact that the long-term average heat flux through the internal and external surfaces differed substantially, most likely due to a phase transition of the water accumulated in the untreated specimens during the WDR protocol. Indeed, the 3C4R model assumes a closed system and therefore it cannot explain a heat loss due to the energy absorbed from the system when the water evaporates (latent heat) and leaves the system indefinitely. As a consequence, vectors of parameters ($\theta$) of the 3C4R model with large $C_2$ values had a high posterior probability distribution since this large thermal capacitance can act as a large heat sink to try to account for the heat entering the specimen through the internal HFP but not leaving through the external one over the analysis period. Specifically, in wet conditions, the central thermal mass estimates were up to two order of magnitude higher and the U-values were always lower than in dry conditions, which is physically not plausible. Additionally, the condition number of the model substantially increased for the analysis in the wet period, indicating structural local identifiability issues in the model.

The 3C3R model was designed as an alternative to the 3C4R one to overcome the issues identified above. By using the internal heat flux and in-cavity temperature observations to fit the model, it allows heat losses due to the phase transition of the water accumulated in the specimen in wet conditions, which can be estimated a posteriori as the difference between the heat through the outer leaf predicted by the model and that measured by the external HFP. With the 3C3R model, the internal heat flux and in-cavity temperature observations were accurately predicted both in dry and wet conditions for the untreated and treated specimens both in the uninsulated and insulated configuration (Figure 5 and Figure 6 are reported as a representative example for the wet and dry conditions respectively; top location for the untreated and uninsulated specimen). Additionally, the predictions of the temperature of all three thermal masses had daily cycles in all configurations, as it would be expected (Figure 5 and Figure 6, as an example).
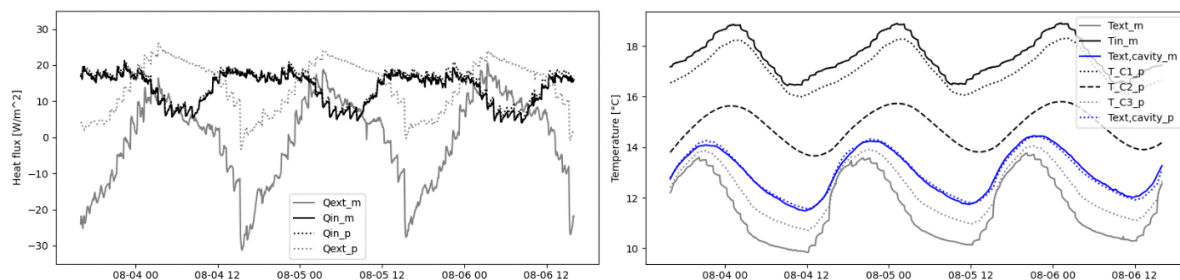


**Figure 5.** Internal and external heat flux (left) and temperature (right) measurements (indicated as _m) and model predictions (indicated as _p) in wet conditions using the 3C3R model (untreated specimen).
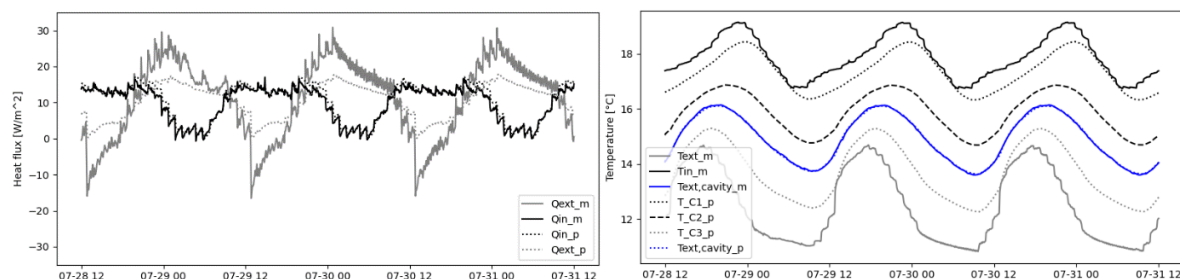


**Figure 6.** Internal and external heat flux (left) and temperature (right) measurements (indicated as _m) and model predictions (indicated as _p) in dry conditions using the 3C3R model (untreated specimen).

Most importantly, the 3C3R model predicted a higher than measured heat flux for the untreated specimen (both uninsulated and insulated) in wet condition (Figure 5, as an example), where the

difference can be ascribed to the latent heat lost due to phase transition. Conversely, the predicted and measured heat flux had a comparable trend for all specimens in dry conditions (Figure 6 and Figure 7 left, as an example) and the treated specimen in wet conditions (Figure 7 right, as an example), both in the uninsulated and insulated configuration. This corroborated the hypothesis that the peculiar behaviour observed for the 3C4R model was related to the unmeasured heat transfer due to phase transition.
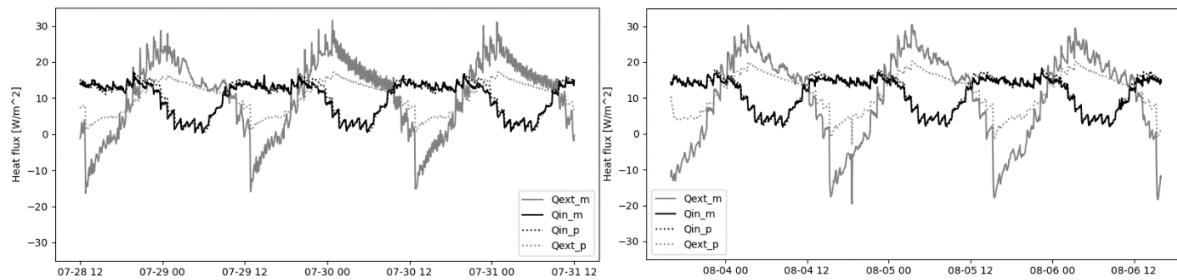


**Figure 7.** Internal and external heat flux measurements (indicated as _m) and model predictions (indicated as _p) in dry (left) and wet (right) conditions using the 3C3R model (treated specimen).

A summary of the U-value estimates and associated systematic measurement error (quantified according to the method described in [13]) obtained in all configurations using the 3C3R model is illustrated in Figure 8.
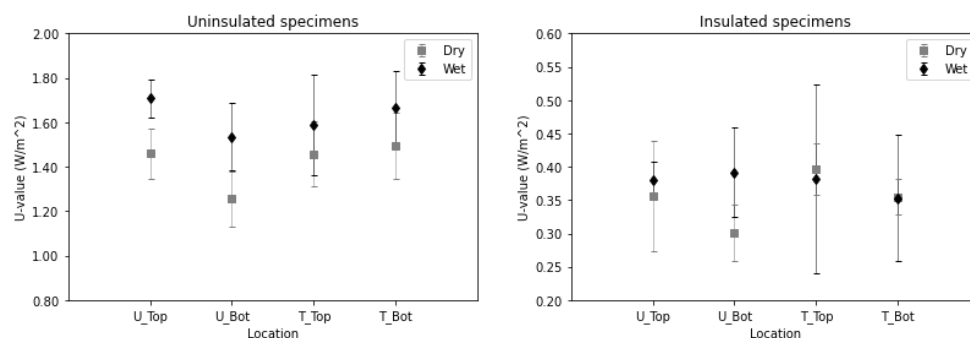


**Figure 8.** U-value estimates (mean±SD) for the 3C3R model in dry and wet conditions for the untreated (indicated as U) and treated (indicated as T) specimens in the uninsulated (left) and insulated (right) configuration.

U-values for the uninsulated cavity-wall specimen in dry conditions ranged between 1.26-1.49 W/m$^2$K, while U-values in wet conditions ranged between 1.54-1.71 W/m$^2$K, all within one standard deviation (Figure 8, left). Therefore, for the uninsulated configuration the U-values in dry conditions were consistently lower than in wet conditions, although always within the margin of error.

As expected, thermal insulation played the main role in the improvement of thermal transmittance as the U-values were significantly reduced when the specimens were insulated with EPS grey beads (Figure 8, right). U-values in dry conditions ranged between 0.30-0.40 W/m$^2$K (generally within one standard deviation), while U-values in wet conditions ranged between 0.35-0.39 W/m$^2$K (all within one standard deviation). All estimates were in line (to the second decimal figure) with the U-value calculated according to the ISO 9869-1:2014 [12] average method.

A percentage U-value increase was observed as a consequence of WDR in the uninsulated configuration, with slightly lower increase (9 and 12%) for the treated specimens compared to the untreated ones (17 and 22%). Similarly, a U-value increase was observed for insulated untreated specimens (7 and 30%), while no increase occurred for the treated ones. The results suggest a negligible efficacy of waterproofing surface treatments as strategies for the reduction of heat transfer within the element. Moreover, the U-value increase between dry and wet conditions indicates that water

penetration occurred in both the treated and untreated cavity-wall specimens. However, the fact that no substantial latent heat and water evaporation effects were predicted through the external leaf of the treated specimens seems to suggest that the application of waterproofing products may affect the evaporative and drying mechanisms.

While promising, the results should be regarded with caution due to the limited sample size, the good state of conservation of the specimens, and the fact that the variation was usually within the associated measurement error. Given the extreme wetting scenario implemented during the laboratory testing, the effects observed are also likely to be more limited in situ. Further laboratory and in-situ studies will be needed to corroborate the initial insights gained with this research on the impact of WDR on the thermophyiscal performance of walls in exposed areas and the effects of water-repellent agents on moisture transfer mechanisms.

## 4. Conclusions

This research investigated the effects of WDR on the thermophysical performance of uninsulated and insulated cavity walls and its degradation as the element is wettened. Laboratory testing was carried out on two cavity-wall specimens, one of which coated with a waterproofing treatment on the external surface. Heat flux and temperature measurements were collected before and after a high wind-driven rain exposure (based on the literature review in [5]). The data collected were analysed using a Bayesian framework to estimate the thermophysical properties of the elements under different conditions (i.e. dry and wet, uninsulated and insulated). The heat transfer through the walls was modelled by means of lumped-thermal-mass models.

U-values estimates were obtained with a 3C3R model fitted with internal heat flux and in-cavity temperature observations. The U-value estimates in wet and dry conditions were compared to evaluate the themophysical performance degradation due to water accumulation in the element. While a slightly lower U-value increase was observed for the treated uninsulated specimens compared to the untreated ones, the results suggest a negligible efficacy of strategies only focussed at minimising the wetting of the element (such as waterproofing treatments) with the aim of improving thermal performance. The U-value increase between dry and wet conditions indicated that water penetration occurred in both the treated and untreated cavity-wall specimens. As expected, thermal insulation played a major role in the improvement of thermal transmittance as the U-values were significantly reduced for both treated and untreated specimens.

The estimates obtained from dynamic lumped-thermal-mass models within a Bayesian framework seem to suggest that the application of waterproofing products may affect the evaporative and drying mechanisms as no substantial latent heat and water evaporation effects were observed through the external leaf of the treated specimen. In particular, a comparison between the 3C3R model (fitted with the internal heat flux and in-cavity temperature observations) and a 3C4R model (fitted with both internal and external heat flux observations) identified the presence of a phase change mechanism (evaporation) in the untreated specimen, which was not observed in the treated specimen.

Given the limited sample size, the good state of conservation of the specimens (not aiming at replicating common construction defects and building detailing), and the extreme wetting scenario implemented during the WDR testing protocol, further laboratory and in-situ studies are needed to corroborate the initial insights gained within this research. Additional aspects to be considered in future work are the variability of old weathered bricks compared to new ones (as used in this research), the possible effects of residual moisture from the building process or previous WDR events, and possible impact of glued EPS beads on the thermophysical performance and moisture and water transport within the structure (as opposite to the loose beads used here).

The use of a dynamic Bayesian framework allowed to gain further insights into the hygrothermal performance of the specimens (e.g., detection of water evaporation for the untreated wet walls), while obtaining U-values in line with the commonly used average method. The analysis showed that building-physics experience and care are needed for a correct evaluation and interpretation of results obtained with the dynamic method to identify potential issues with the models and suitable refinements. The

limited invasiveness and enhanced level of understanding of the hygrothermal performance of the building fabric gained with the dynamic method may make it very promising as a diagnostic tool including for traditional buildings subject to high water penetration, for example to evaluate their state and conservation to inform retrofit strategies, moisture risk assessment, and quality assurance over time after intervention.

**References**
[1]    Department of Energy and Climate Change (DECC) 2013 Estimates of home insulation levels in Great Britain [online] https://www.gov.uk/government/statistical-data-sets/estimates-of-home-insulation-levels-in-great-britain
[2]    Van Goethem S, Van Den Bossche N, and Janssens A 2015 Watertightness assessment of blown-in retrofit cavity wall insulation *Energy Procedia* **78** pp. 883–8
[3]    Blocken B and Carmeliet J 2004 A review of wind-driven rain research in building science *J Wind Eng Ind Aerodyn* **92**(13) pp. 1079-1130
[4]    Gori V, Biddulph P and Elwell C A 2018 A Bayesian dynamic method to estimate the thermophysical properties of building elements in all seasons, orientations and with reduced error *Energies* **11**(4) pp. 802
[5]    Weeks C, Sutton A and Bassett T 2021 Waterproofing cavity walls to allow insulation in exposed areas: Appendix A (Wall Analysis). BEIS Research Paper Number 2021/017. [online] https://www.gov.uk/government/publications/waterproofing-cavity-walls
[6]    Marincioni V, Gori V and Altamirano-Medina H 2021 Identifying suitable inputs for the moisture risk assessment of waterproofed cavity walls with surface waterproofing treatment *Proc. 8th Int. Building Physics Conf. (IBPC 2021), 25-27 August 2021, Copenhagen*
[7]    Hukseflux, HFP01 Heat Flux Plate [online] http://www.hukseflux.com/product/hfp01
[8]    EU*(copper base)/EUS (st. st. base), Thermistor [online] https://www.eltekdataloggers.co.uk/sensors_temperature.php
[9]    DataTaker, DT85 Data logger [online] http://www.datataker.com
[10]   Campbell Scientific, CR23X Data logger [online] https://www.campbellsci.com/cr23x
[11]   D'Ayala D, Aktas Y D and Zhu H 2021 Waterproofing cavity walls to allow insulation in exposed areas: Appendix E (WDR Testing). BEIS Research Paper Number 2021/017. [online] https://www.gov.uk/government/publications/waterproofing-cavity-walls
[12]   ISO 9869-1:2014. Thermal insulation -- Building elements -- In-situ measurement of thermal resistance and thermal transmittance. Part 1: Heat flow meter method.
[13]   Gori V and Elwell C A 2018 Estimation of thermophysical properties from in-situ measurements in all seasons: Quantifying and reducing errors using dynamic grey-box methods *Energy Build* **167** pp. 290-300